

# Individualized Prediction of COVID-19 Adverse outcomes with MLHO

Hossein Estiri,<sup>1,2,3</sup> Zachary H. Strasser,<sup>1,3,4</sup> Shawn N. Murphy<sup>1,2,3,4,5</sup>

<sup>1</sup> Laboratory of Computer Science, Massachusetts General Hospital, Boston, MA, 02144, USA.

<sup>2</sup> Research Information Science and Computing, Mass General Brigham, Somerville, MA, 02145, USA.

<sup>3</sup> Harvard Medical School, Boston, MA, 02115, USA.

<sup>4</sup> Department of Biomedical Informatics, Harvard Medical School, Boston, MA, 02115 USA.

<sup>5</sup> Department of Neurology, Massachusetts General Hospital, Boston, MA, 02114, USA.

Corresponding Author: Hossein Estiri

Postal address: MGH Laboratory of Computer Science, 50 Staniford Street, Suite 750, Boston, MA 02114, USA.

E-mail: [hestiri@mgh.harvard.edu](mailto:hestiri@mgh.harvard.edu)

Phone: 617-726-2463

## Abstract

The COVID-19 pandemic has devastated the world with health and economic wreckage. Precise estimates of the COVID-19 adverse outcomes on individual patients could have led to better allocation of healthcare resources and more efficient targeted preventive measures. We developed MLHO (pronounced as melo) for predicting patient-level risk of hospitalization, ICU admission, need for mechanical ventilation, and death from patients' past (before COVID-19 infection) medical records. MLHO is an end-to-end Machine Learning pipeline that implements iterative sequential representation mining and feature and model selection to predict health outcomes. MLHO's architecture enables a parallel and outcome-oriented calibration, in which different statistical learning algorithms and vectors of features are simultaneously tested and leveraged to improve prediction of health outcomes. Using clinical data from a large cohort of over 14,000 patients, we modeled the four adverse outcomes utilizing about 600 features representing patients' before-COVID health records. Overall, the best predictions were obtained from extreme and gradient boosting models. The median AUC ROC for mortality prediction was 0.91, while the prediction performance ranged between 0.79 and 0.83 for ICU, hospitalization, and ventilation. We broadly describe the clusters of features that were utilized in modeling and their relative influence on predicting each outcome. As COVID-19 cases are re-surfing in the U.S. and around the world, a Machine Learning pipeline like MLHO is crucial to improve our readiness for confronting the potential future waves of COVID-19, as well as other novel infectious diseases that may emerge in the near future.

## Introduction

The global spread of COVID-19, the disease caused by SARS-CoV-2, has resulted in the loss of around 700,000 lives. Repercussions of the pandemic have wreaked havoc on the economy, sending billions of people into lockdown to flatten the curve for the healthcare systems and resulting in record-high unemployment around the world. The American Hospital Association estimates a total four-month financial impact of over \$200 billion in losses for the U.S. healthcare systems as a result of cancelled hospital services (e.g., cancelled non-elective surgeries and outpatient treatment) due to the COVID-19 pandemic and COVID-19 hospitalizations.<sup>1</sup> Our inability to provide precise estimates of the COVID-19 outcomes such as death, hospitalization, and need for ICU and ventilation has contributed to lost opportunities for saving lives with personalized preventive measures and making smart resource allocation plans. Although our inability to predict was partly due to the novelty of the disease, the critical question is: do we have the data and technology to predict?

Over the past decade, the U.S. federal government has made extensive investments to institute meaningful use of electronic health record (EHR) systems. Clinical data in EHRs, however, are still complex and have important quality issues, impeding their leverage to address pressing health issues that require rapid response. Nevertheless, biomedical researchers are increasingly applying data mining and Machine Learning techniques to clinical data for predicting health outcomes.

Recent studies have shown that COVID-19 disease severity and mortality are associated with a number of comorbidities including cardiovascular disease, diabetes mellitus, hypertension, chronic lung disease, cancer, chronic kidney disease, and obesity, and demographics including age, sex, and race/ethnicity.<sup>2-8</sup> A number of Machine Learning (ML) models have been developed to predict susceptibility in the general population, the likelihood of a positive diagnosis in a patient with symptoms, and prognosis in those with the disease.<sup>9</sup> Many of these models are based on a combination of demographics, comorbidities, symptoms, and biomarkers,<sup>10-15</sup> and use data from relatively small cohorts of COVID-19 patients. Jiangfeng et al,<sup>10</sup> for example, performed a logistic regression analysis on 299 patients that identified age, lymphocyte count, lactate dehydrogenase, and oxygen saturation as independent predictors for mortality. Jiang et al,<sup>15</sup> used data from 53 patients to develop ML models to identify elevated alanine aminotransferase (ALT), the presence of myalgias, and an elevated hemoglobin as the most predictive features for disease severity, achieving approximately 70-80% accuracy in modeling COVID-19 mortality. Huang et al<sup>11</sup> examined clinical data from 125 COVID-19 patients and identified the presence of comorbidities, increased respiratory rate, elevated C-reactive protein, and elevated lactate dehydrogenase as independently associated with a worse prognosis. While the inclusion of vital signs and biomarkers in these models may be highly predictive of some adverse outcomes of COVID-19 infection, they are typically measured after the patient has already started to show signs of the disease and may be at a point that is too late for a useful intervention.

Estiri et al. recently introduced the transitive Sequential Pattern Mining (tSPM) along with a dimensionality reduction algorithm, MSMR, and showed that together, the algorithms can successfully predict different health outcomes.<sup>16,17</sup> The goal in tSPM is to mine temporal data representations from clinical data for application in downstream ML. The number of transitive sequential representations is quadratic in the number of records, and thus create dimensionality issues. To address this, the MSMR algorithm -- short form stands for Minimize Sparsity, Maximize Relevance, applies high performance dimensionality reduction (Figure 1). It takes the initial set of N features mined by the tSPM algorithm and provides a list of <400 features, through a 3-step process including frequency-based and information-based (mutual information, and joint mutual information) filtering of a large number of features.<sup>16,17</sup>

We adapt the tSPM temporal representation mining and MSMR dimensionality reduction algorithms, and make adjustments to architect an end-to-end ML pipeline that enables iterative feature and algorithm selection to predict health outcomes (MLHO, pronounced as melo). MLHO offers an architecture that enables a parallel outcome-targeted calibration of the features and algorithms. The goal in MLHO is to mine relevant data representations from past clinical records and select the most efficient algorithmic solution for accurately predicting future health outcomes. As COVID-19 cases are rising again in many areas of the world, being able to provide personalized predictions of its adverse outcomes that are directly connected to the healthcare systems' responsiveness and mortality can be game-changing. In this study, we focus on predicting four outcomes (hospitalization, ICU, ventilation, and death) in patients with a verified COVID-19 infection, using their past medical records. Using about 600 features mined from patients' past medical records (before contracting COVID-19), we trained and tested predictive models that estimate risks of hospitalization, ICU admission, need for mechanical ventilation, and death.

## Method

Implementation of the MLHO pipeline is depicted in Figure 1. MLHO mines both sequential (temporal) and raw data representations from clinical data and performs iterative feature and algorithm selection in a 2-step evaluation process. MLHO's architecture enables a parallel outcome-targeted calibration of the features and algorithms, in which different statistical learning algorithms and vectors of features are simultaneously tested and leveraged to improve prediction of health outcomes. The four adverse outcomes of interest in this study reflect a hypothetical sequential spectrum of outcome severity in patients with verified COVID-19 infection, ranging from hospitalization to ICU admission, to need for mechanical ventilation, and ultimately to death (Hospitalization → ICU → Ventilation → Death).

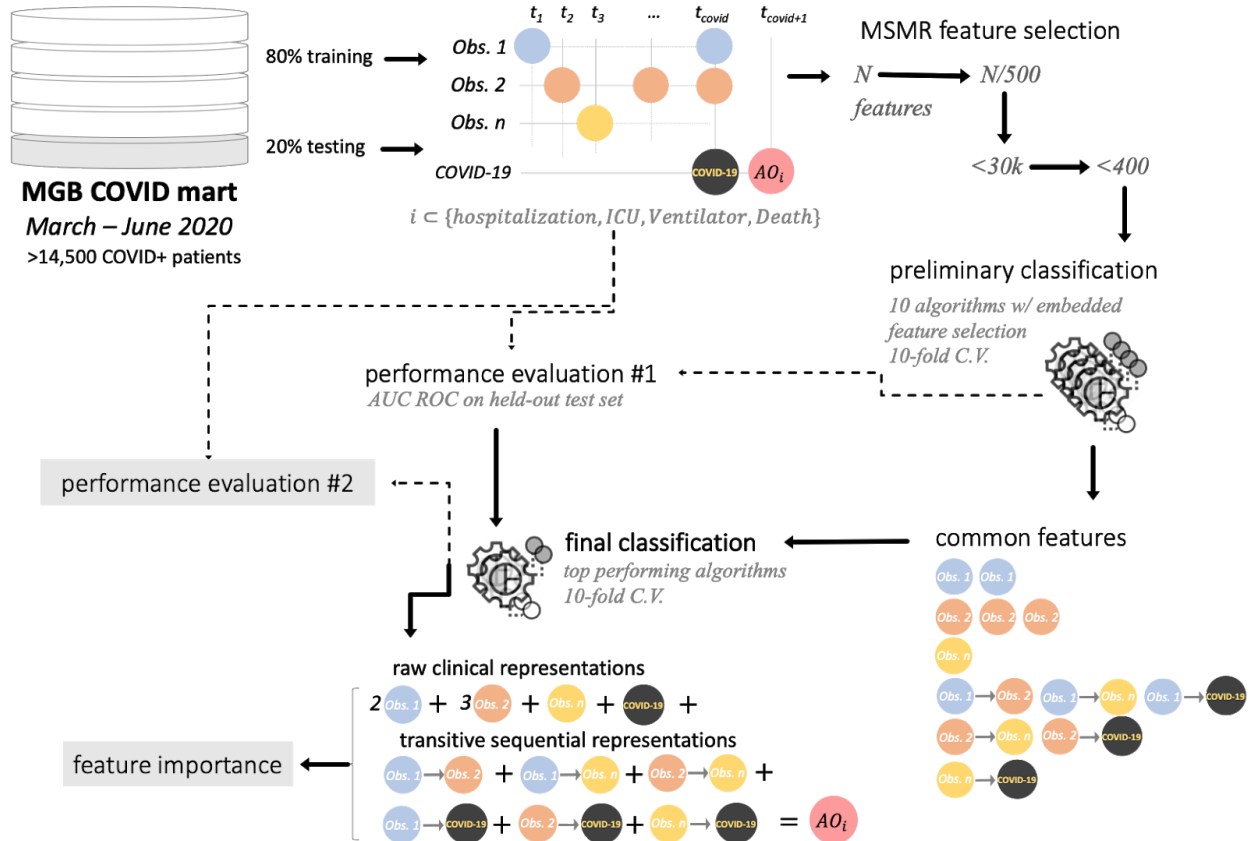


**Figure 1.** Implementation of the MLHO pipeline for predicting COVID-19 adverse outcomes

## Experimental Setup

We used electronic health records data from over 14,500 patients with a confirmed case for COVID-19 between March and May 2020 and who had at least 1 year of medical history with Mass General Brigham (MGB), since 2016. Table 1S presents general demographic information about the study cohort. For each patient, we only included clinical records from 14 days prior to the positive COVID-19 test date. This temporal buffer ensures that no COVID-19-related medical conditions are included in the model as a risk factor. The use of data for this study was approved by the Mass General Brigham Institutional Review Board (2020P001063).

We randomly split the data with an 80-20 training-to-testing ratio. We iterated the train-test sampling 10 times to account for possible patient population differences caused by the sampling. We used the tSPM algorithm to mine temporal sequential representations. Given a list of clinical records  $R_1, R_2, \dots, R_n$  for patient  $p$  at times  $t_{i1} \leq t_{i2} \leq \dots \leq t_{ik_i}$ , the tSPM algorithm mines all avector of transitive sequential patterns  $X_{ij}$  from possible pairs of distinct records  $(R_i, R_j)$ , where  $i \neq j \leq n$ , by setting  $r_{ij}$  (as samples of random variable  $X_{ij}$  for patient  $p$ ) to be 1 if  $k_i \geq 1, k_j \geq 1$  and  $t_{i1} \leq t_{j1}$ , and 0 otherwise. We also mined raw representations from the clinical

data, which are composed of all clinical records. To obtain a count of the raw records, for each patient  $p$ , we sum the frequency of  $k_1, k_2, \dots, k_n$ , as samples of a random variable  $X_i$ .

On the training sets, we performed feature and algorithm selection and the final predictive modeling. We feed the combined representations  $X' = (X_i \cup X_{ij})_{i \neq j}$  to the feature selection step.

## Iterative feature and algorithm selection

Unlike other studies that begin with a limited set of hypothetical risk factors, we took a primarily inductive approach to selecting clinical representations for predicting the risk of adverse outcomes in COVID-19 patients. First, we apply a filter method for feature selection, using a computational algorithm that minimizes sparsity and maximizes relevance (MSMR<sup>16,17</sup>). Step 1 in MSMR is to cut the initial combined vector of representations  $X'$  to those that were observed in fewer than 0.2 percent of the patients. On the remaining representations, step 2 in MSMR computes the mutual information with the outcome variable  $Y = (y_1, \dots, y_i)$ , which in this study includes labels for hospitalization, ICU, ventilation, and death. Mutual information,<sup>18,19</sup> in this case, measures the amount of information that each remaining representation contains about the outcome. Given the joint probability distribution  $P_{X'Y}(x', y)$ , the mutual information between them is denoted as  $I(X' : Y)$  is:

$$\sum_{x'y} P_{X'Y}(x', y) \times \log \frac{P_{X'Y}(x', y)}{P_{X'}(x') \times P_Y(y)}$$

We cut the remaining representations from  $X'$  by ranking based on the mutual information coefficient, and update  $X'$  to a list of around 30,000 representations with the highest mutual information. In the third and final step, MSMR computes the joint mutual information (JMI)<sup>20</sup> score for the updated vector of remaining representations,  $X'$ . The algorithm starts with a set  $S$  containing the top feature according to mutual information, then iteratively adds to  $S$  the features maximizing the joint mutual information score

$$J_{jmi}(X') = \sum_{X^* \in S} I(X'X^*; Y)$$

Where the random variable  $X'X^*$  corresponds to the joint distribution of  $X'$  and  $X^*$ . As a result, JMI also takes into account the redundancy between the features – i.e., reducing multicollinearity among covariates. Second, we combine the feature selection with a preliminary evaluation of algorithms for the prediction task.

Using the <400 features identified by the MSMR algorithm, we train a set of preliminary classification algorithms that perform embedded feature selection. The preliminary classification serves two goals. First, we screened features used in those algorithms to compile a list of the common features used for modeling the 4 outcomes. Second, during each sampling iteration, we computed the Area Under the Receiver Operating Characteristic Curve (AUC ROC) on the held-out test sets to evaluate the algorithms' performance for predicting the outcome labels. We used 10-fold cross-validation to train the prediction algorithm -- therefore, a 72-8-20,

train-evaluation-test split. We tested 10 classification algorithms -- bartMachine: Bayesian Additive Regression Trees,<sup>21,22</sup> Stacked AutoEncoder Deep Neural Network (dnn), Stochastic Gradient Boosting (gbm),<sup>23,24</sup> glmboost: Boosted Generalized Linear Model, eXtreme Gradient Boosting (xgb)<sup>25</sup> with DART booster (xgbDART),<sup>26</sup> linear model solver (xgbLinear), tree learning (xgbTree), model-averaged Neural Network (avNNet), Elastic-Net regularized generalized linear model (glmnet),<sup>27,28</sup> and Oblique random forest (ORFlog).<sup>29</sup>

## Final classification

The iterative feature and algorithm (preliminary classification) selection results in a set of common features and a ranking of classification algorithms. Using the top algorithms (by AUC ROC) and the common features, we perform a final round of classification training with 10 train-test sampling iteration and 10-fold cross-validation. We also measured a model-specific feature importance/influence metric in the final modeling rounds.

As we shall reveal in the results, the gbm algorithm was one of the top 2 performing algorithms. As a result, we computed the relative feature influence metrics from the final gbm models to measure features' importance. In the gbm model, boosting estimates  $\hat{F}(X)$  as an 'additive' expansion of the form

$$\hat{F}(X) = \sum_{m=0}^M \beta_m h(X; a_m)$$

Where the expansion coefficients  $\{\beta_m\}_0^M$  and the base learner's --  $h(X; a)$  -- parameters  $\{a_m\}_0^M$  are jointly fit to the training data in a feedforward process. A regression tree model specializes the base learner  $T_m(X; \{R_{jm}\}_1^J)$  partitions the feature space into  $J$  disjoint regions  $\{R_{jm}\}_{j=1}^J$  to predict a different constant value for each.<sup>30</sup> The relative influence (or contribution),  $I_j^2$  averages the improvement made by each variable when it is permuted from all trees in which the given variable was incorporated.<sup>30,31</sup> In an additive tree model, the relative influence measure is provided by Friedman and Meulman (2003)

$$I_j^2 = \frac{1}{M} \sum_{m=1}^M I_j^2(T_m)$$

where  $I_j^2(T)$  is the measure of relevance for a single tree  $T$ .<sup>32</sup>

We summarize and report the AUC ROCs from the final models as well as the features' relative influence values.

## Results

Table 1S provides a summary of demographic characteristics of the patients. We found that among racial/ethnic groups, the rate of hospitalization, ICU admission, and ventilation was highest among African American/black individuals. The overall mortality rate was three percent, and white individuals had the highest rate (3.9 percent) compared to other racial/ethnic groups. Compared to females, male COVID-19 patients had a significantly higher chance of hospitalization, ICU admission, ventilation, and mortality. While the average age in the cohort of

COVID-19 patients was 49.5, the average age of patients who were hospitalized, admitted to ICU, or needed mechanical ventilation was between 61 and 62. The average age of mortality in COVID-19 patients was much higher at 77 years (Table 1S).

Figure 2 summarizes the sequential scenarios in which the four adverse outcomes are observed in COVID-19 patients. Overall, in more than 75 percent of the patients we did not observe any adverse outcomes. Approximately 13 percent of patients were discharged after hospitalization. The cumulative probability of patients needing to be admitted to the ICU was less than eight percent, which sorted in a declining order of sequential events from four percent to 1.4 percent for Hospitalized → ICU → Discharged, Hospitalized → ICU → Ventilation → Discharged, Hospitalized → ICU → Ventilation → Died. This order supports our general hypothesis about the severity spectrum. Of the three percent overall chance of mortality, 2.5 percent fall into the sequential scenarios of Hospitalized → ICU → Ventilation → Died and Hospitalized → Died (without ICU/Ventilation).

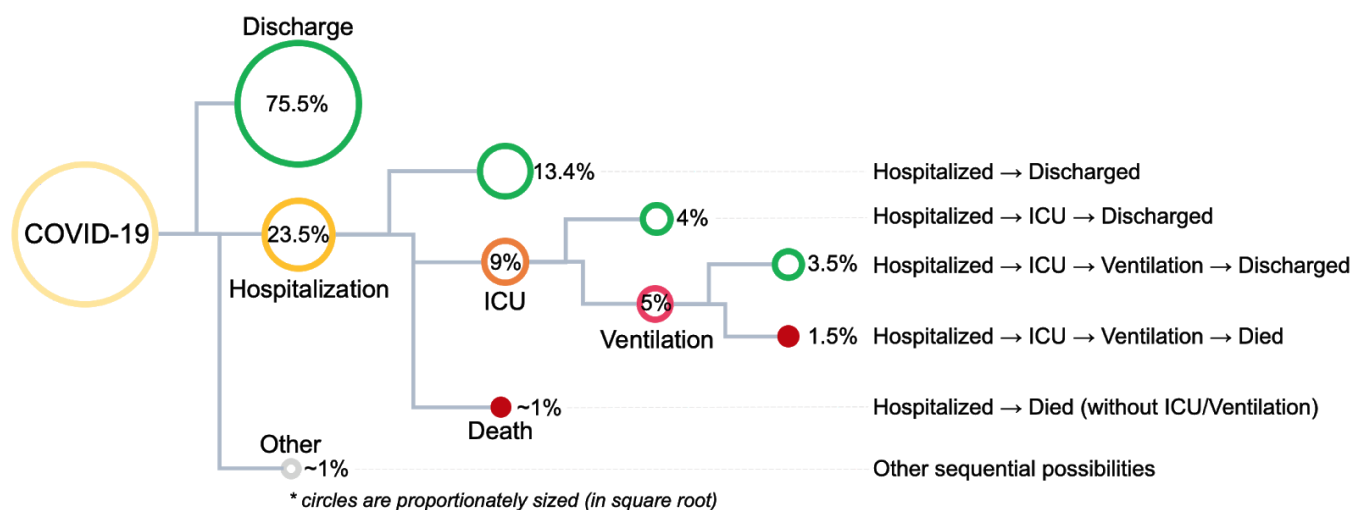


**Figure 2.** Probability of the sequential scenarios for outcomes after COVID-19 infection.

## Iterative feature and algorithm selection

MLHO mined over 60 thousand raw (e.g., diagnosis/medication/procedure codes) and 160 million transitive sequential (e.g., medication → diagnosis) representations. Through the iterative feature selection, these features were shrunk to over 2,300 representations, about 900 of which were raw features and about 1,400 were transitive sequential features. As described in the methods, both MSMR filter method and embedded methods (while training preliminary classification algorithms) were utilized in iterative sampling of train-test data. The other outcome of this step was identification of the top predictive algorithms. Figure 3 illustrates the AUC ROC results obtained from the 10 algorithms for estimating the risk of hospitalization. We found that two Boosting algorithms obtained the best overall results: the Stochastic Gradient Boosting (gbm) -- a.k.a., gradient boosting machine -- and the eXtreme Gradient Boosting (xgb) with DART booster (xgbDART)





\*median AUC ROC values are printed

Algorithms from right to left: bartMachine: Bayesian Additive Regression Trees, dnn: Stacked AutoEncoder Deep Neural Network, gbm: Stochastic Gradient Boosting, glmboost: Boosted Generalized Linear Model, xgbDART: eXtreme Gradient Boosting (xgb) with DART booster, linear model solver (xgbLinear), tree learning (xgbTree), avNNet: model-averaged Neural Network, glmnet: Elastic-Net regularized generalized linear model, and ORFlog: Oblique random forest.

**Figure 3.** AUC ROC result of the preliminary classification step for predicting hospitalization.

## Final modeling

We fed the shrunken feature set (with ~2,300 features) to the two top algorithms for the final model training -- with 10 iterative train-test sampling and 10-fold cross-validation, which means for each outcome, we trained 20 final models. We picked the top 10 models, by AUC ROC. Table 1 presents the median, standard deviation, and the best AUC ROC values obtained from the final models for each outcome. Overall, the median AUC ROCs was the best for mortality, while it ranged near the 0.8 threshold for hospitalization, ICU, and ventilation. Among the top 10 models, the gbm algorithm was the best algorithm for hospitalization and ICU, and the xgbDART was the best algorithm for predicting the need for mechanical ventilation.

**Table 1.** The classification performance of the final models

outcome	median	sd*	best	gbm	xgbDART
<b>Mortality</b>	0.912	0.002	0.915	3	7
<b>Hospitalization</b>	0.801	0.002	0.807	10	0
<b>ICU</b>	0.787	0.003	0.792	10	0
<b>Ventilation</b>	0.831	0.003	0.838	0	10

\* standard deviation

## Features' relative influence

Because the relative influence measures from the gradient boosting models are relative, by default the largest value is assigned to 100, and the remaining values are scaled accordingly.<sup>30</sup> Using only the non-zero relative influence values resulted in a final set of 603 features that were used for predicting at least one of the outcomes. Table 2S provides the list of features with their median and interquartile range values of relative influence by outcome.

The features were then grouped under nine different clusters that correspond to comorbidities and demographics that have been associated with poor outcomes in COVID-19 by the Center for Disease and Control<sup>33</sup>. The categories are cardiovascular disease, chronic renal disease, chronic lung disease, neurological disorder, diabetes mellitus, other chronic illness, age, sex, and race/ethnicity. The "Other chronic illness" cluster includes comorbidities such as hypertension, hyperlipidemia, hypothyroidism, obstructive sleep apnea, and obesity.

Table 2 is a sample of features that were assigned to two of these disease clusters. The features used include diagnoses, medications, laboratory tests, imaging studies, and procedures. Diagnoses can easily be identified as a subtype of a particular category. For example, "Type 2 diabetes mellitus with diabetic nephropathy" is grouped with diabetes mellitus and "Unspecified dementia without behavioral disturbance" is grouped with neurological disorder. Medication labels are assigned to a specific cluster if the medication is exclusively used for that disease. For example, "metformin" is assigned to the diabetes mellitus cluster because it is primarily used for treating diabetes mellitus. However, in many cases a medication can be used for multiple diseases and cannot be easily grouped with a specific cluster. If a medication cannot be attributed to a specific cluster, it was left unassigned.

For the sequential features, if one of the two components in the sequence was related to a disease cluster; the whole sequence was assigned to the corresponding disease. Laboratory tests, imaging studies and procedures on their own are not associated with a particular disease. But they were assigned to particular disease clusters if they were in sequence with another label that was specific to a disease cluster. For example, the sequence "CT Head → Altered Mental Status" was associated with a neurological disorder because it includes the diagnosis "Altered Mental Status".

**Table 2.** Sampling of select features used for identifying specific disease clusters (in this case Diabetes Mellitus and Neurological Disorder)

<b>Disease Cluster</b>	<b>Diabetes Mellitus</b>	<b>Neurological Disorder</b>
<b>Diagnosis</b>	-Type 2 diabetes mellitus with diabetic chronic kidney disease -Type 2 diabetes mellitus with diabetic nephropathy -Unspecified Essential Hypertension-> Type 2 Diabetes Mellitus without complications	-Unspecified dementia without behavioral disturbance -Cerebral infarction, unspecified -Essential (primary) hypertension -> Unspecified dementia without behavioral disturbance
<b>Medication</b>	-Metformin -Sodium Chloride 0.9% Injection Syringe -> Insulin Lispro 100 unit/ml subcutaneous	-Acetaminophen -> Unspecified dementia without behavioral disturbance
<b>Laboratory Test</b>	-Blood count; complete (CBC), automated and automated differential WBC count -> Injection, insulin, per 5 units	Natriuretic peptide -> Altered Mental Status, unspecified -Basic Metabolic Panel (BMP) -> Unspecified dementia without behavioral disturbance
<b>Imaging Study</b>	-Type II Diabetes mellitus or unspecified type, not stated as uncontrolled, without mention of complication -> Electrocardiogram, routine ECG	-Electrocardiogram, routine ECG -> Altered mental status, unspecified -CT Head -> Altered mental status, unspecified
<b>Procedure</b>	-Emergency Department Visit for Evaluation and Management -> Insulin	-

After assigning features to specific disease clusters the mean relative variable influence for the cluster was determined for each of the outcomes. Table 3 shows the relative influence of each of the clusters for determining hospitalization, ventilation, ICU admission, and death. Age was excluded from the table as it is by far the most predictive for each of the outcomes with a mean relative variable influence of 99.99. Excluding age, the most influential clusters for the prediction of death are chronic lung disease, sex, neurological disorder, and race/ethnicity. The top predictors for ICU admission are sex, chronic renal disease, other chronic illness, and diabetes mellitus. The top predictive clusters for ventilation are sex, diabetes mellitus, race, and chronic renal disease. While for hospitalization, sex, race/ethnicity, other chronic illness, and diabetes mellitus, are the most predictive clusters.

**Table 3.** Mean relative influence of the features associated with hospitalization, ventilation, ICU admission, and death

Hospitalization	Var. Inf*	Ventilation	Var. Inf	ICU	Var .Inf	Death	Var. Inf
Sex (Female)	4.52	Sex (Female)	18.04	Sex (Female)	9.57	Chronic Lung Disease	3.61
Race/Ethnicity	3.93	Diabetes Mellitus	4.21	Chronic Renal Disease	1.89	Sex (Female)	3.44
Other Chronic Illness	0.45	Race/Ethnicity	3.65	Other Chronic Illness	1.48	Neurological Disorder	3.27
Diabetes Mellitus	0.44	Chronic Renal Disease	1.71	Diabetes Mellitus	1.36	Race**	3.06
Cardiovascular Disease	0.41	Other Chronic Disease	1.63	Chronic Lung Disease	0.74	Chronic Renal Disease	2.16
Chronic Renal Disease	0.20	Chronic Lung Disease	1.33	Cardiovascular Disease	0.37	Cardiovascular Disease	1.84
Neurological Disorder	0.04	Cardiovascular Disease	0.95			Diabetes Mellitus	1.52
		Neurological Disorder	0.51			Other Chronic Illness	1.31

\* Mean relative variable influence -- relative influence values are scaled between 0 to 100.

\*\* The race category is an aggregation of races White and Black or African American. Details are available in Table 2S.

## Discussion

Using the MLHO pipeline, we developed models for predicting risks of hospitalization, ICU admission, need for mechanical ventilation, and death for patients infected with COVID-19. We were able to model the four adverse outcomes with about 600 features from patients' past medical records, before they contracted COVID-19. MLHO can leverage the past medical records in clinical repositories to quickly develop predictive models with acceptable accuracy.

One could envision different applications for such predictions. For example, we could aggregate MLHO's predictions based on a population's expected rates of infection during a pandemic, to better allocate healthcare resources in preparation for a surge in cases. It would also help allocate the number of critical care nurses and doctors, ventilators, hospital beds, and supplies in the case of a resurgence of the pandemic.

Being able to predict the four outcomes can also create possibilities for better preventive measures. For instance, healthcare systems and regional health authorities can use predicted outcomes to identify patients who might be at higher risks and plan for preventive measures such as alerting the patients' primary care providers to prioritize healthcare maintenance visits in order to make sure the patients are up to date on immunizations and health care screening. There could also be an in-person discussion of the importance of taking precaution against contracting COVID-19. The estimated risks provided by MLHO can also help stratify the most at-risk from already known vulnerable populations such as those living in nursing homes, subacute rehabilitation centers, and homeless shelters for potential high risk.

We found that the average age for patients who died was about 77, whereas the average age for hospitalization, ventilation, and ICU admission was around 61. This shows that the patients hospitalized and having critical illness interventions (such as an ICU admission or intubation) in general have a younger age. One possible explanation for this discrepancy is that many of the younger patients with these interventions may survive. This suggests that the younger patients who get intensive therapies such as ventilation or admission into the ICU, see an improvement compared to the older patients who may have less improvement with such therapies.

The relative influence of specific disease clusters for different outcomes suggests certain diseases may have increased predictive value for determining adverse outcomes. Age is by far the best predictor for an adverse outcome. It is far more influential of the prediction than any other comorbidity or demographic including severe diseases such as congestive heart failure, end stage renal failure, or dementia. Another interesting trend between outcomes is that chronic illness (hypertension, hypothyroidism, and obesity) and diabetes mellitus are relatively more influential predictors for hospitalization, ICU admission, and need for ventilation than they are for death. However, the comorbidity with the best prediction for death is chronic lung disease. This could suggest that intensive therapies such as ventilation and admission into the ICU, may improve the outcome of patients with common comorbidities such as hypertension and hyperlipidemia but they do not have as beneficial of an impact on patients with chronic lung disease.

Findings of this study can exhibit limitations due to the potential availability of noise in outcome labels. Outcomes such as hospitalization, ICU admission, and ventilation can be difficult to uniformly measure since they can be correlated with healthcare utilization. For example, hospitalization could be due to a heart failure exacerbation and the COVID-19 diagnosis is only incidentally discovered, but unrelated to the hospitalization.

## Conclusion

The COVID-19 pandemic has had devastating health and economic impacts across the globe. Being able to predict adverse outcomes that directly impact the capacity of healthcare systems in a timely manner can lead to better allocation of healthcare resources and more efficient targeted economic and preventive measures. MLHO's architecture enables a parallel outcome-targeted calibration of the features and algorithms, in which different statistical learning algorithms and vectors of features are simultaneously tested and leveraged to improve prediction of health outcomes. As the COVID-19 cases are re-surg-ing around the world, a pipeline like MLHO is crucial to improve our readiness for confronting not only the potential future waves of COVID-19, but also other novel infectious diseases that may emerge.

## Funding

This work was funded through the National Human Genome Research Institute grants R01-HG009174.

## References

1. Hospitals and Health Systems Face Unprecedented Financial Pressures Due to COVID-19. <https://www.aha.org/guidesreports/2020-05-05-hospitals-and-health-systems-face-unprece-dented-financial-pressures-due>.
2. Wu, Z. & McGoogan, J. M. Characteristics of and important lessons from the coronavirus disease 2019 (COVID-19) outbreak in China: summary of a report of 72 314 cases from the Chinese Center for Disease Control and Prevention. *JAMA* **323**, 1239–1242 (2020).
3. Petrilli, C. M. *et al.* Factors associated with hospital admission and critical illness among 5279 people with coronavirus disease 2019 in New York City: prospective cohort study. *BMJ* **369**, m1966 (2020).
4. Zhou, F. *et al.* Clinical course and risk factors for mortality of adult inpatients with COVID-19 in Wuhan, China: a retrospective cohort study. *Lancet* **395**, 1054–1062 (2020).
5. Liang, W. *et al.* Cancer patients in SARS-CoV-2 infection: a nationwide analysis in China. *Lancet Oncol.* **21**, 335–337 (2020).

6. Covid, C. D. C. *et al.* Preliminary estimates of the prevalence of selected underlying health conditions among patients with coronavirus disease 2019—United States, February 12–March 28, 2020. *MMWR Surveill. Summ.* **69**, 382 (2020).
7. Lighter, J. *et al.* Obesity in Patients Younger Than 60 Years Is a Risk Factor for COVID-19 Hospital Admission. *Clin. Infect. Dis.* **71**, 896–897 (2020).
8. Williamson, E. J. *et al.* OpenSAFELY: factors associated with COVID-19 death in 17 million patients. *Nature* (2020) doi:10.1038/s41586-020-2521-4.
9. Wynants, L. *et al.* Prediction models for diagnosis and prognosis of covid-19 infection: systematic review and critical appraisal. *BMJ* **369**, m1328 (2020).
10. Jianfeng, X. *et al.* Development and external validation of a prognostic multivariable model on admission for hospitalized patients with COVID-19. <https://www.medrxiv.org/content/medrxiv/early/2020/03/30/2020.03.28.20045997.full.pdf> (2020).
11. Huang *et al.* Prognostic factors for COVID-19 pneumonia progression to severe symptom based on the earlier clinical features: a retrospective analysis. doi:10.1101/2020.03.28.20045989.
12. Yan, L. *et al.* Prediction of criticality in patients with severe Covid-19 infection using three clinical features: a machine learning-based prognostic model with clinical data in Wuhan. *MedRxiv* (2020).
13. Sarkar, J. & Chakrabarti, P. A Machine Learning Model Reveals Older Age and Delayed Hospitalization as Predictors of Mortality in Patients with COVID-19. doi:10.1101/2020.03.25.20043331.
14. McRae, M. P. *et al.* Clinical Decision Support Tool and Rapid Point-of-Care Platform for Determining Disease Severity in Patients with COVID-19. *medRxiv* (2020) doi:10.1101/2020.04.16.20068411.

15. Jiang, X. *et al.* Towards an artificial intelligence framework for data-driven prediction of coronavirus clinical severity. *CMC: Computers, Materials & Continua* **63**, 537–551 (2020).
16. Estiri H, Strasser ZH, Klann JG, McCoy TH Jr., Wagholikar KB, Vasey S, Castro VM, Murphy ME, Murphy SN. Transitive Sequencing Medical Records for Mining Predictive and Interpretable Temporal Representations. *Patterns* (2020).
17. Hossein Estiri, Sebastien Vasey, Shawn N Murphy. Transitive sequential pattern mining for discrete clinical data. in *Artificial Intelligence in Medicine* (ed. Martin Michalowski, R. M.) (Springer, 2020).
18. Shannon, C. & Weaver, W. Recent contributions to the mathematical theory of communication. *The mathematical theory of communication* **1**, 1–12 (1949).
19. Cover, T. M. & Thomas, J. A. *Elements of Information Theory*. (John Wiley & Sons, 2012).
20. Battiti, R. Using mutual information for selecting features in supervised neural net learning. *IEEE Trans. Neural Netw.* **5**, 537–550 (1994).
21. Chipman, H. A., George, E. I. & McCulloch, R. E. BART: Bayesian additive regression trees. *Ann. Appl. Stat.* **4**, 266–298 (2010).
22. Kapelner, A. & Bleich, J. bartMachine: Machine Learning with Bayesian Additive Regression Trees. *Journal of Statistical Software, Articles* **70**, 1–40 (2016).
23. Friedman, J. H. Stochastic gradient boosting. *Comput. Stat. Data Anal.* **38**, 367–378 (2002).
24. Greenwell, B., Boehmke, B., Cunningham, J., Developers, G. B. M. & Greenwell, M. B. Package ‘gbm’. *R package version 2*, (2019).
25. Chen, T. & Guestrin, C. XGBoost: A Scalable Tree Boosting System. in *Proceedings of the 22nd ACM SIGKDD International Conference on Knowledge Discovery and Data Mining* 785–794 (Association for Computing Machinery, 2016).
26. Vinayak, R. K. & Gilad-Bachrach, R. DART: Dropouts meet Multiple Additive Regression



- Trees. in *Proceedings of the Eighteenth International Conference on Artificial Intelligence and Statistics* (eds. Lebanon, G. & Vishwanathan, S. V. N.) vol. 38 489–497 (PMLR, 2015).
27. Friedman, J., Hastie, T. & Tibshirani, R. Regularization paths for generalized linear models via coordinate descent. *J. Stat. Softw.* **33**, 1 (2010).
  28. Simon, N., Friedman, J. & Hastie, T. A Blockwise Descent Algorithm for Group-penalized Multiresponse and Multinomial Regression. *arXiv [stat.CO]* (2013).
  29. Menze, B. H., Kelm, B. M., Splitthoff, D. N., Koethe, U. & Hamprecht, F. A. On Oblique Random Forests. in *Machine Learning and Knowledge Discovery in Databases* 453–469 (Springer Berlin Heidelberg, 2011).
  30. Friedman, J. H. & Meulman, J. J. Multiple additive regression trees with application in epidemiology. *Stat. Med.* **22**, 1365–1381 (2003).
  31. Friedman, J. H. Greedy Function Approximation: A Gradient Boosting Machine. *Ann. Stat.* **29**, 1189–1232 (2001).
  32. Breiman, L., Friedman, J., Stone, C. J. & Olshen, R. A. *Classification and regression trees*. (CRC press, 1984).
  33. Covid, C. D. C. & Team, R. Severe outcomes among patients with coronavirus disease 2019 (COVID-19)—United States, February 12–March 16, 2020. *MMWR Morb. Mortal. Wkly. Rep.* **69**, 343–346 (2020).